

AD-A081 976

MICHIGAN TECHNOLOGICAL UNIV HOUGHTON DEPT OF METALLU--ETC F/6 20/11
DUCTILE FRACTURE UNDER MULTIAXIAL STRESS STATES BETWEEN PAIRS 0--ETC(U)
NOV 79 R J BOURCIER, D A KOSS N00014-76-C-0037

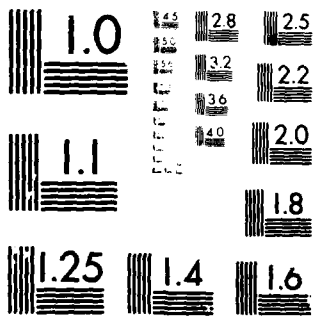
UNCLASSIFIED

TR-11

ML

10-1
40
200 1/17

END
DATE
FILMED
4-80
DTIC



MICROCOPY RESOLUTION TEST CHART
NATIONAL BUREAU OF STANDARDS-1963-A

1
TECHNICAL REPORT No. 11

To

LEVEL II

12
B.S.

THE OFFICE OF NAVAL RESEARCH

CONTRACT No. N00014-76-C-0037

AD A081976

DUCTILE FRACTURE UNDER MULTIAXIAL STRESS STATES
BETWEEN PAIRS OF HOLES

1473 in 2nd

By

DTIC
ELECTE
MAR 13 1980
S D C

R. J. BOURCIER AND D. A. KOSS

DEPARTMENT OF METALLURGICAL ENGINEERING

MICHIGAN TECHNOLOGICAL UNIVERSITY

HOUGHTON, MICHIGAN U.S.A.

DO NOT FILE COPY

80 3 10 050

REPRODUCTION IN WHOLE OR IN PART IS PERMITTED FOR ANY PURPOSE
OF THE UNITED STATES GOVERNMENT. DISTRIBUTION OF THIS DOCUMENT
IS UNLIMITED.

DUCTILE FRACTURE UNDER MULTIAXIAL STRESS STATES

BETWEEN PAIRS OF HOLES

R. J. Bourcier and D. A. Koss
Department of Metallurgical Engineering
Michigan Technological University
Houghton, Michigan 49931 U.S.A.

As a means of examining ductile fracture under multiaxial stress and strain states, the deformation and fracture between pairs of holes has been studied in a 7075 Al alloy. The test technique, which is unique, utilizes tensile samples each with a pair of holes through the thickness. The holes are sufficiently close (two hole diameters apart) so as to concentrate slip between them, and the local states of stress and strain can be controlled by the orientation of the holes to the stress axis.

The influence of hole orientation on the strain at fracture has been determined in the 7075 Al alloy in the T6 as well as T0 tempers. Fracture occurs by flow localization between the holes and very little hole growth occurs, especially in the T6 condition. Fractography indicates a transition in fracture appearance with hole orientation with dimpled fracture predominating, but the degree of shear fracture increases as the pair of holes become more inclined to the stress axis. A modification of the Bridgeman analysis is used as a description of the approximate state of stress between the holes as a function of the hole orientation. The results indicate that the criterion for ductile fracture depends on both the state of stress and the strain state, but the functional dependence could not be determined. The results are also discussed as a crude model for void coalescence in ductile fracture.

Accession For	Microfilm
MS. G. 4.1	
Doc. TAB	
Unannounced	
Justification	
By	
Distribution	
Availability Codes	
Avail and/or	
Dist special	
Dist	A

Introduction

Ductile fracture cannot be fully understood until its functional dependence on stress as well as strain states is established. In recent years, many studies have analyzed ductile fracture on a microscopic scale using void initiation and void growth processes based on dislocation models, continuum plasticity analyses, and experimental studies of soft, ductile alloys (for reviews, see refs. 1-5). From a macroscopic standpoint, the importance of the hydrostatic or mean stress on ductile fracture is well established.^{6,7} However, there have been relatively few experimental efforts to establish macroscopic criteria for ductile fracture occurring under multiaxial stress and strain states.⁸⁻¹⁰ Furthermore, the stress and strain states should be particularly important in influencing the fracture of high strength alloys. Such alloys typically exhibit relatively low work hardening rates and comparatively small strain rate sensitivities, making them susceptible to flow localization processes between voids. It is reasonable to expect that such flow localization processes, while quite unlike those occurring in sheet metals, should be nonetheless sensitive to the stress/strain states, thus affecting fracture.

As a means of establishing ductile fracture criteria under multiaxial stress conditions and of crudely modeling void link-up in the ductile fracture of high strength alloys, the present research examines deformation and fracture between pairs of holes. The test technique, which is unique, utilizes tensile samples each with a pair of holes drilled through the thickness. The holes are sufficiently close (two hole diameters apart) so as to concentrate slip between them, and the local strain components are measured with the aid of a square grid of lines. The orientation of the holes to the tensile axis can be systematically varied, and thus the states of stress and strain between the holes may be controlled. Fracture of the tensile sample occurs when the ligament between the holes fails. A series of tests as a function of hole orientation therefore permits one to

subject the material in the ligament between the holes to different stress states and to measure the state of strain at fracture. A principal problem is to obtain the state of stress in the fully plastic ligament between the holes. In the present study, we deal with this problem in an approximate manner by adopting the Bridgeman analysis for notched tensile samples. This allows an analysis of the data in terms of hydrostatic or mean stress/equivalent strain criteria for fracture. The results also contain implications regarding void link-up, and these will be discussed. Results are presented for a 7075 Al alloy both in the T6 and T0 tempers.

Experimental

The experimental data is obtained using a pair of holes tensile sample shown in Fig. 1. In this study, the holes in Fig. 1 are 0.5mm diameter, the centers of the holes are 1.5mm apart, and they are drilled through a gage section 6.4mm thick and 12.8mm wide. A square grid of lines spaced 0.4mm apart was scribed onto the sample such that the grid axes correspond to the x and y axes in Fig. 1. All tests were performed at a constant displacement rate such that the nominal engineering strain rate was $.005 \text{ sec}^{-1}$.

The presence of the grids and the initial dimensions of the section of the sample containing the holes permits an accurate determination of the average state of strain in the ligament between the holes. In terms of the axes in Fig. 1, the shear strain γ_{xy} can be measured directly from the grid at any time prior to fracture. The normal strain components ϵ_{xx} and ϵ_{zz} (see Fig. 1 for definition of axes) are measured by recording edge to edge spacings of the holes along the center to center plane between the holes during the test (which yields ϵ_{xx}) and by measuring the thickness of the ligament before and after fracture (from which ϵ_{zz} at fracture is determined). Macrophotography is used to determine ϵ_{xx} and γ_{xy} prior to fracture. As expected, these strain components are linearly

dependent on tensile strain. Therefore the state of strain at fracture is obtained by measuring ϵ_{xx} and γ_{xy} periodically as a function of tensile strain and extrapolating a small amount (<1% strain) to the tensile fracture strain ϵ_f of the specimen. The third normal strain component in the plane of the fracture, ϵ_{yy} , is then calculated by assuming constant volume.

The material used in this study was a 7075 Al alloy (in wt. %: 1.60 Cu, 2.46 Mg, 5.78 Zn, .26 Fe, .19 Cr, and .10 Si) obtained courtesy of the Aluminum Corporation of America in the form of 6.4mm thick plate. After specimen preparation according to Fig. 1, the samples were heat treated to either the T6 temper (solution-treated at 465°C for three hours, water quenched, and aged at 120°C for twenty-four hours) or a T0 temper (425°C for 1 hour, furnace cool at 28°C/hr to 230°C plus 6 hours at 230°C). In both cases, the grain size is approximately 0.1 mm.

Experimental Results

The dependence of the tensile strain and the strain components at the point of fracture of the ligament between the holes on the hole orientation is shown in Fig. 2 (T6 temper) and Fig. 3 (T0 temper). It should be noted that the schematic insert in Figs. 2 and 3 depicting the sample is not drawn to scale as in reality the holes are located ≈ 10 hole diameters from the sides of the gage section. Figs. 2 and 3 clearly indicate that the strain components ϵ_{ij} at fracture are strongly dependent on hole orientation with a transition occurring from a state of strain characterized by normal strains at $\theta = 0^\circ$ to predominantly a single shear strain component γ_{xy} ($= \gamma_{yx}$) at $\theta = 45^\circ$. The tensile strain to fracture ϵ_f [based on the central section of the gage length, ≈ 15 hole diameters long, which contains the holes] is also very dependent on hole orientation, showing a minimum at $\theta = 30^\circ$ for both tempers, see Figs. 2 and 3. This behavior occurs not only in the 7075 Al alloy tested here, but also in 1.5mm thick Ti-8Al-1Mo-1V sheet tested with the pairs of holes sample configuration.

Figure 4 shows a profile of the ligament just prior to macroscopic fracture. Relatively little hole growth occurs prior to fracture, especially in the T6 condition (note: Fig. 4 is of the T0 condition which failed more gradually enabling this micrograph to be obtained). Fig. 4 also shows the formation of voids between the holes and suggests their link-up by a shear process. As such, Fig. 4 is very similar to the classic micrographs of Cox and Low¹¹ and Forsythe and Smale¹² showing void link-up in a 4340 steel and BSL 64 Al, respectively. Examination of the fracture surface profiles between the holes in other T0 and T6 samples indicate that fracture at $\theta \leq 60^\circ$ occurs on a plane similar to that being developed in Fig. 4. This plane is close to but not identical with the plane connecting the axes of the holes.

Fractography, as seen in Fig. 5, indicates a transition in fracture appearance with hole orientation. At $\theta = 0^\circ$ (i.e., holes oriented perpendicular to the stress axis), the fracture surface is characterized by void formation and coalescence typical of tensile fracture. The dimples are elongated parallel to the plate surface, and inclusions, also typical of 7075 Al, are seen in Fig. 5a. However, beginning with the $\theta = 15^\circ$ samples, the fracture surfaces also contain regions of shear-type fracture in addition to the dimpled fracture. An example of this mixed dimpled-shear fracture is shown in Fig. 5b for the $\theta = 30^\circ$ sample. The extent of the shear areas increases with increasing θ from about 20% at $\theta = 15^\circ$ to a maximum of about 40% of the fracture surface at $\theta = 60^\circ$ in the T6 sample. While the $\theta \neq 0^\circ$ samples fail by mixed mode I and mode II displacements, the dimples present in the inclined-hole fracture surfaces are not significantly elongated in the shear direction.

Discussion

A. Macroscopic Considerations

Any analysis of the experimental data must recognize the multiaxial nature of both the strain state and stress state. The nature of the test is such that,

although the condition of plane strain nearly prevails in the T6 material, fracture between the holes occurs under neither plane stress nor, strictly speaking, plane strain. The equivalent plastic strain in the ligament at fracture can be calculated directly from the experimental plastic strain components ϵ_{ij} and is:

$$\bar{\epsilon}_f = \left[\frac{2}{9} \{ (\epsilon_{xx} - \epsilon_{yy})^2 + (\epsilon_{yy} - \epsilon_{zz})^2 + (\epsilon_{zz} - \epsilon_{xx})^2 \} + \frac{1}{3} \gamma_{xy}^2 \right]^{1/2} \quad (1)$$

Determination of the state of stress in the ligament at fracture presents considerably more difficulty. To do this, we assume that the Bridgeman analysis⁶ for the stress state* in a necked tensile specimen can be modified by resolving the nominal axial stress σ_a on the present test sample into a shear stress component σ_{xy} and the normal stresses σ_{yy} and σ_{xx} . The stress state in the ligament between the holes can be roughly estimated by taking into account the reduced area of this section and by assuming that the σ_{yy} component ($\sigma_a \cos^2 \theta$) generates triaxial stresses in the ligament according to the Bridgeman analysis. Assuming plane strain, this analysis gives the following crude estimate of the normal stresses between a pair of holes of radius R and whose surfaces are spaced 2a apart in a gage section W wide:

$$\left. \begin{aligned} \sigma_{xx} &\geq \sigma^* \cos^2 \theta \ln A \\ \text{but } \sigma_{xx} &\leq \sigma^* \cos^2 \theta \ln A + \sigma_a \sin^2 \theta \\ \sigma_{yy} &\approx \sigma^* \cos^2 \theta [1 + \ln A], \quad \sigma_{zz} = \frac{1}{2} (\sigma_{xx} + \sigma_{yy}) \\ \sigma_{xy} &\approx \left(\frac{W}{W - 4R \cos \theta} \right) \sigma_a \cos \theta \sin \theta \\ \text{and } \sigma_{xz} &= \sigma_{yz} = 0, \quad \text{where } A = 1 + \frac{1}{2} \frac{a}{R} \left(1 - \frac{x^2}{a^2} \right) \\ \text{and } \sigma^* &= \left(\frac{W}{W - 4R \cos \theta} \right) \frac{\sigma_a}{\left\{ \left(1 + \frac{2R}{a} \right)^{1/2} \ln \left[1 + \frac{a}{R} + \left(\frac{2a}{R} \right)^{1/2} \left(1 + \frac{a}{2R} \right)^{1/2} \right] - 1 \right\}} \end{aligned} \right\} \quad (2)$$

In the present case, the pair of holes geometry is such that $a/R = 2$ in eqns. 2. The σ_{xx} component reflects the fact that, far from the holes ($y \gg 0$), the term ($\sigma_a \sin^2 \theta$) exists because of the rotation of the stress axis. While there is some contribution to σ_{xx} between the holes from this term, especially as $\theta \rightarrow 90^\circ$, that contribution must be less than $\sigma_a \sin^2 \theta$ since $\sigma_{xx} = 0$ at $x = a$ and $y = 0$.

There is support for the use of eqns. 2 to describe roughly the stress state between the holes. In Fig. 6, the lower limit of the present analysis (i.e., $\sigma_{xx} = \sigma^* \cos^2 \theta \ln A$) is compared to the specific plane strain case analyzed by Oh and Kobayashi.¹⁴ Finite element techniques were used to determine the stress-strain states

*Clausing has modified Bridgeman's original work,¹³ but for the circular configuration and hole geometry used here the values of σ_H/σ as determined by the two analyses should be within $\leq 20\%$ of each other.

between an array of holes at $\theta = 45^\circ$ for holes spaced 4 hole diameters apart in which case the $(W/W-4R\cos\theta)$ term is 1.25. Unfortunately, no other orientations were examined. The calculations for $\theta = 45^\circ$ predict the presence of a shear band connecting the two holes as well as the hydrostatic tension ratio graphed in Fig. 6. This figure shows the present analysis is in good agreement (<10%) with the ratio of $(\sigma_{xx} + \sigma_{yy})/\bar{\sigma}$ calculated by Oh and Koboyashi except near the surface of the hole where present analysis significantly underestimates (~25%) the stress ratio calculated by Oh and Koboyashi.¹⁴ Under these conditions, Oh and Koboyashi calculate the average equivalent stress in the ligament $\bar{\sigma}$ to be $\bar{\sigma} \approx 1.30 \sigma_y$ (the yield stress) while the present analysis predicts $\bar{\sigma} = 1.25 \sigma_y$. It is interesting to note that both analyses yield the same $((\sigma_{xx} + \sigma_{yy})/\sigma)_{Ave}$ ratio of 0.93. We thus conclude that at $\theta = 45^\circ$ and probably for $0 \leq \theta \leq 60^\circ$, eqns. 2 provides a reasonable estimate of the stress state if $\sigma_{xx} \approx \sigma^* \cos^2\theta \ln A$.

Using the lower limit value for σ_{xx} , Fig. 7 shows the functional dependence of the average mean hydrostatic stress ($\sigma_H = \frac{1}{3} (\sigma_{xx} + \sigma_{yy} + \sigma_{zz})$) calculated for both plane strain and plane stress (for which $\sigma_{zz} = \sigma^* \cos^2\theta \ln A$) and as a function of hole orientation angle θ . It should be obvious from Fig. 7 that there is not a great difference between the two stress states. This is reassuring since the data, particularly for the TO condition, indicate that the prevailing conditions, while close to plane strain, should probably be between those of plane strain and plane stress. As one would expect, Fig. 7 indicates that σ_H decreases substantially with increasing values of θ although it is likely that at $\theta = 60^\circ$, the $\sigma_a \sin^2\theta$ term ignored previously is important and σ_H is larger than that in Fig. 7.

Having experimentally determined the state of strain and crudely estimated the state of stress between the holes as a function of orientation, we now turn to the question of a fracture criteria. It is reasonable in the present case to assume that ductile fracture occurs in the ligament between the holes at a critical combination of equivalent plastic strain $\bar{\epsilon}_f$ and the hydrostatic stress state parameter $\sigma_H/\bar{\sigma}$ at failure initiation. Figure 8 shows the functional dependence

of $\bar{\epsilon}_f$, $\sigma_H/\bar{\sigma}$, as well as the tensile strain to fracture ϵ_f . Careful examination of Fig. 8 indicates that the data does not fit any obvious simple fracture criteria. Clearly the data does not fit either a critical hydrostatic stress or critical strain criteria. Nor can fracture criteria based on either a product: $(\sigma_H/\bar{\sigma})^a \cdot (\bar{\epsilon}_f)^b$ or the sum: $A(\sigma_H/\bar{\sigma}) + B\bar{\epsilon}_f$ to explain the experimental results. Equally unsuccessful are attempts to use the analysis of McClintock^{15,16} for fracture by hole growth and coalescence to explain the observed dependence of fracture strain on hole orientation. Thus, we conclude that there is no apparent fracture criteria which adequately predicts ductile fracture in the ligament between the holes.

B. Microscopic Considerations

Certain qualitative features of the failure process in the test sample appear straightforward and may be significant with regard to the microscopic aspects of ductile fracture. In this Al alloy which is characterized by a relatively high yield strength (≈ 520 MPa) and low work hardening ($d\ln\sigma/d\ln\epsilon \approx .09$), fracture occurs by relatively little hole growth, even at $\theta = 0^\circ$ and especially in the T6 condition. This is readily apparent in Fig. 4 which shows a sample in the much more ductile T0 condition ($\sigma_y \approx 110$ MPa and $d\ln\sigma/d\ln\epsilon \approx .10$). Somewhat similar behavior has been observed in the tensile testing of perforated mild steel sheet.¹⁷ To the extent that these tests model the void link-up process in ductile fracture, this result indicates the potential importance of the link-up of voids by a shear process involving flow localization. That ductile fracture occurs by the possible interventions of plastic instability before complete homogeneous growth and coalescence of holes has also been well recognized by others.^{3,18} However, there is little direct experimental evidence which shows the importance of shear in the fracture between holes.

The sequence of events leading to failure is also clearly indicated. Fig. 4 indicates that voids form between the holes, presumably characterized by

the dimpled regions in Fig. 5. Total separation of the fracture surface occurs when the voids are linked by a flow localization and shear process, giving rise to the shear fracture regions in Fig. 5. Relatively little macroscopic strain occurs between the initiation of the large voids and their subsequent link-up by shear especially in the T6 condition.

SUMMARY

A test technique utilizing tensile samples with pairs of through-thickness holes has been described. This simple test may be utilized to study ductile fracture under a relatively broad combination of multiaxial stress as well as strain states. The corresponding stress state in the ligament between the holes can be reasonably estimated using a modified Bridgeman analysis while the state of strain can be determined experimentally. Results from tests performed on a 7075 Al alloy indicate that fracture occurs by flow localization between the pair of holes with very little hole growth occurring prior to fracture. Although ductile fracture clearly depends on both the state of stress as well as the strain state, attempts to establish a well defined fracture criteria were unsuccessful. The results also suggest the importance of the link-up of voids by a shear localization process, as opposed to exclusively void growth and coalescence, in the ductile fracture of high strength alloys.

ACKNOWLEDGEMENTS

The authors would like to thank Dr. R. Tait for helpful discussions. This program was supported by the Office of Naval Research through Contract No. N00014-76-C-0037.

References

1. I. L. Mogford, *Met. Rev.* 12, 49 (1967).
2. A. R. Rosenfield, *Met. Rev.* 13, 29 (1968).
3. F. A. McClintock in Ductility, (ASM: Metals Park), p. 255, 1968.
4. F. A. McClintock in Fracture, (Academic Press: New York), p. 47, 1971.
5. S. H. Goods and L. M. Brown, *Acta Met.*, 27, 1 (1979).
6. P. W. Bridgeman, Studies in Large Plastic Flow and Fracture, (McGraw-Hill, New York), 1952.
7. H. Ll. Pugh in Irreversible Effects of High Pressure and Temperature on Materials, ASTM STP 374, (ASTM, Philadelphia), p. 68, 1965.
8. J. W. Hancock and A. C. MacKenzie, *J. Mech. Phys. Solids* 24, 147 (1976).
9. A. C. MacKenzie, J. W. Hancock and D. K. Brown, *Eng. Frac. Mech.* 9, 167 (1977).
10. K. Osakada, A. Watadani and H. Sekiguchi, *Bull. Jap. Soc. Mech. Eng.*, 20, 1557 (1977).
11. T. B. Cox and J. R. Low, *Met. Trans.* 5, 1457 (1974).
12. P. J. E. Forsythe and A. C. Smale, *Eng. Frac. Mech.* 3, 127 (1971).
13. D. P. Clausing, *J. Mat'l. JMLSA* 4, 566 (1969).
14. S. I. Oh and S. Koboyashi, in "Theories of Flow and Fracture in Metalworking Processes," Air Force Materials Lab. Report AFML-TR-76-61, May, 1976, p. 61.
15. F. A. McClintock, S. M. Kaplan, and C. A. Berg, *Int. J. Frac. Mech.* 2, 614 (1966).
16. F. A. McClintock, *J. Appl. Mech.* 35, 363 (1968).
17. M. Nagumo, *Acta Met.* 21, 1661 (1973).
18. P. F. Thomason, in Prospects of Fracture Mechanics, (Nordhoff Int. Pub.: Holland), p. 3, 1974.

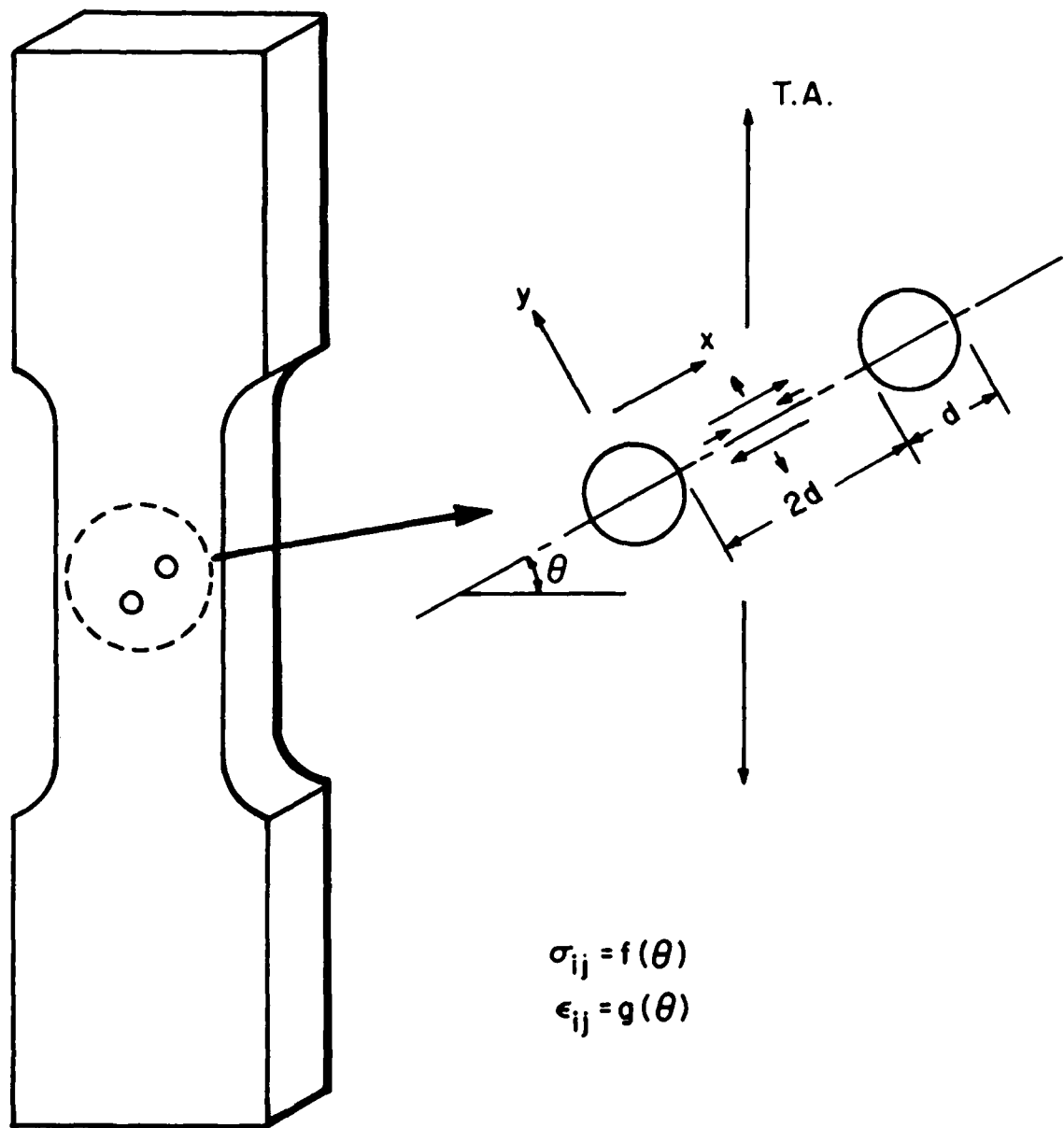


Fig. 1. A schematic diagram of the pair-of-holes tensile sample. Note that the holes are centrally located in a gauge section $\approx 25 d$ wide and $\approx 75 d$ long.

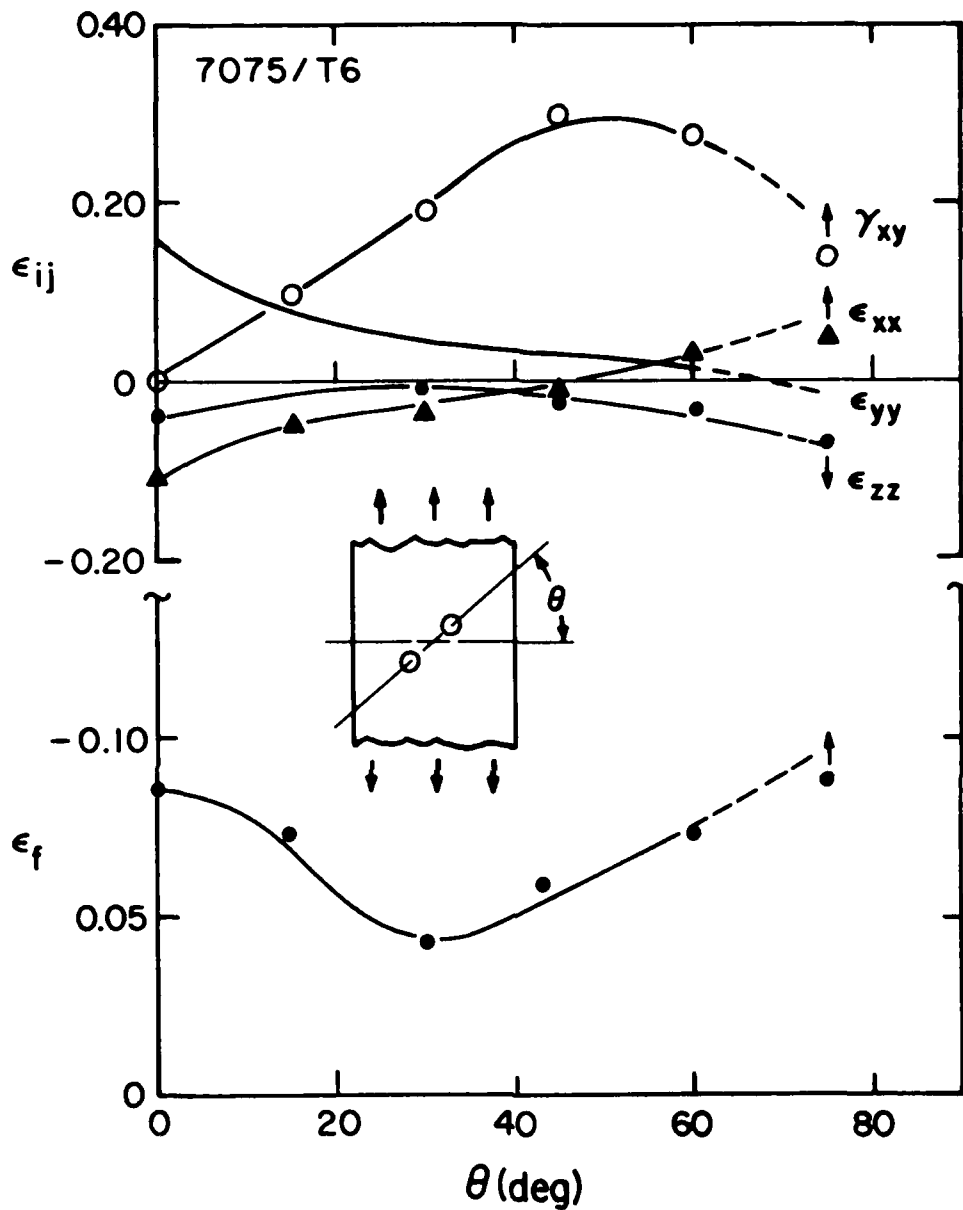


Fig. 2. The dependence of the strain components ϵ_{ij} at fracture of the ligament between the holes and of the tensile strain to fracture ϵ_f on hole orientation θ for a 7075 Al alloy in the T6 temper. The magnitude of ϵ_f is based on the central section of the gauge length, $\sim 15 d$ long, containing the pair of holes.

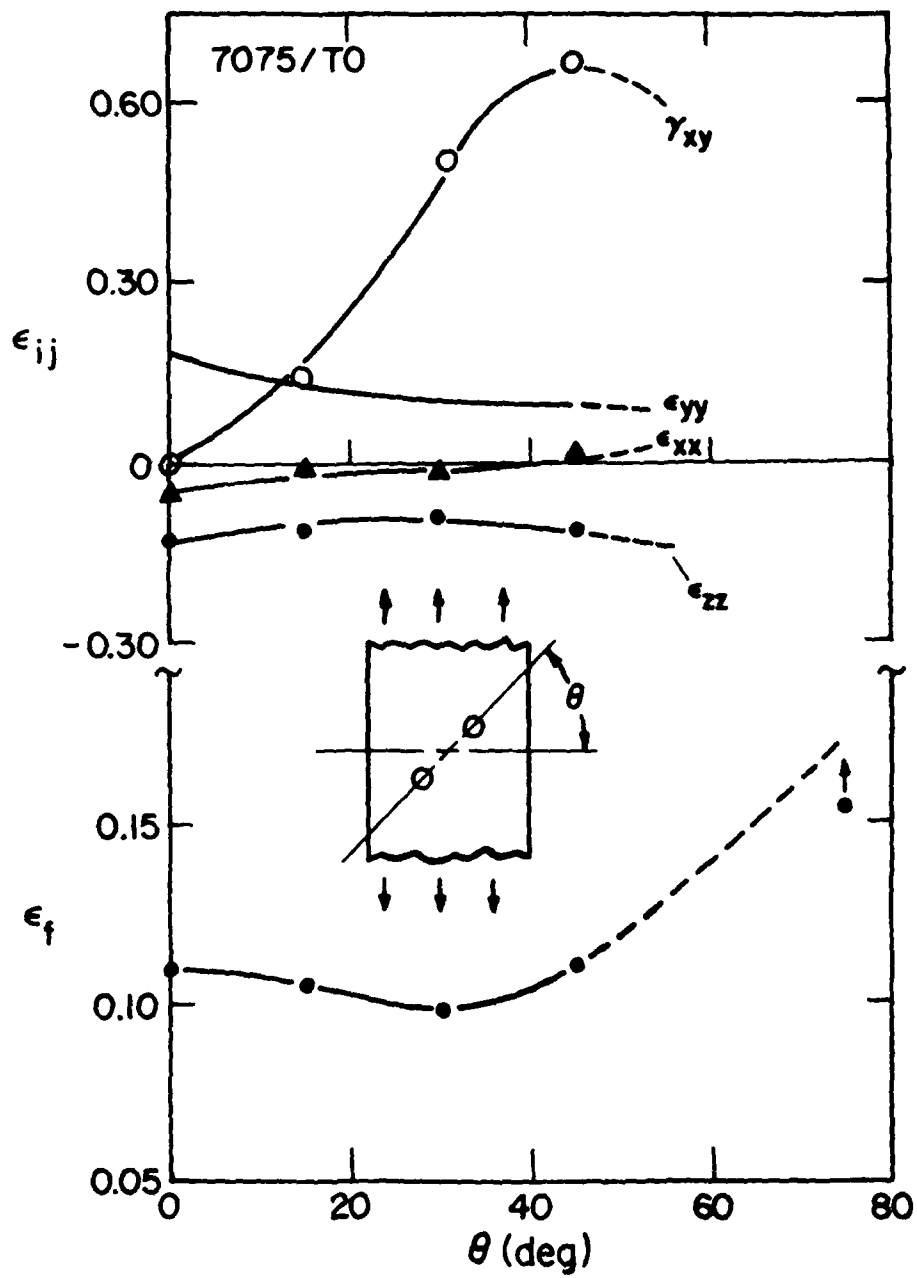


Fig. 3. The dependence of the strain components ϵ_{ij} at fracture of the ligament between the holes and of the tensile strain to fracture ϵ_f on hole orientation θ for a 7075 Al alloy in the T0 temper.

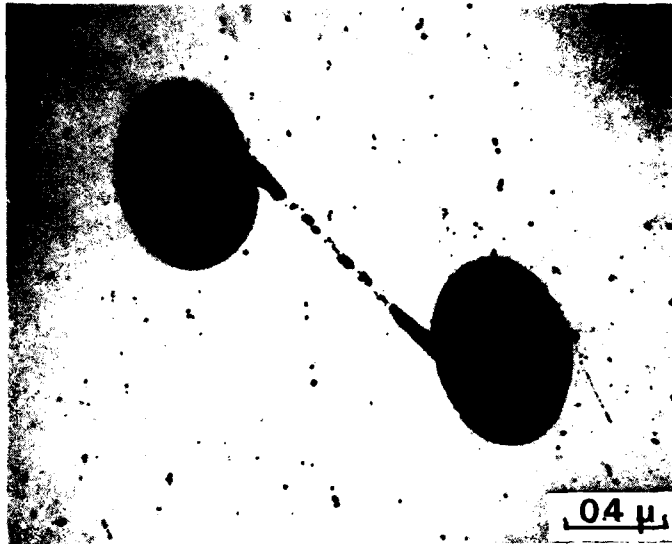


Fig. 4. An optical micrograph showing the profile of a sheet of voids forming prior to fracture of the ligament between the pair of holes in a 7075 Al alloy in the T0 temper. The tensile axis is vertical.

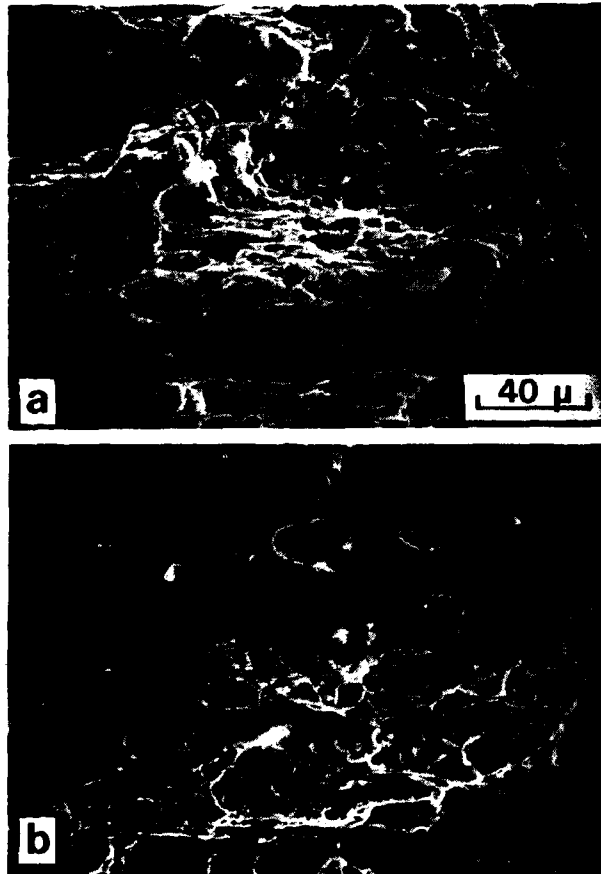


Fig. 5. Electron micrographs showing the fracture surface of the ligament between the holes for the 7075 Al in the T6 temper: (a) at $\theta = 0^\circ$ and (b) at $\theta = 30^\circ$.

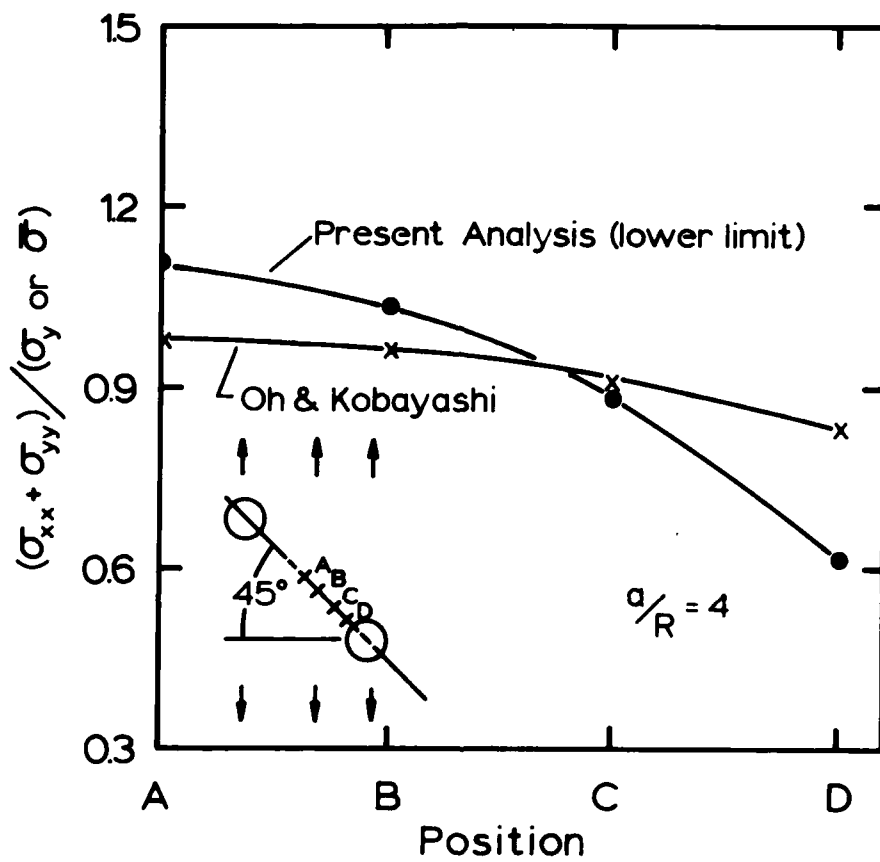


Fig. 6. The stress ratio $(\sigma_{xx} + \sigma_{yy}) / (\sigma_y \text{ or } \bar{\sigma})$ as a function of the position between a pair of holes for the specific condition illustrated. The present analysis is based on $\sigma_{xx} = \sigma^* \cos^2 \theta$ in A with σ^* being calculated at the yield stress of the gage section away from the holes (i.e., $\sigma_a = \sigma_y$). The Oh and Kobayashi data¹⁴ is at 10% strain in the ligament between the holes and is also for 7075 Al/T6.

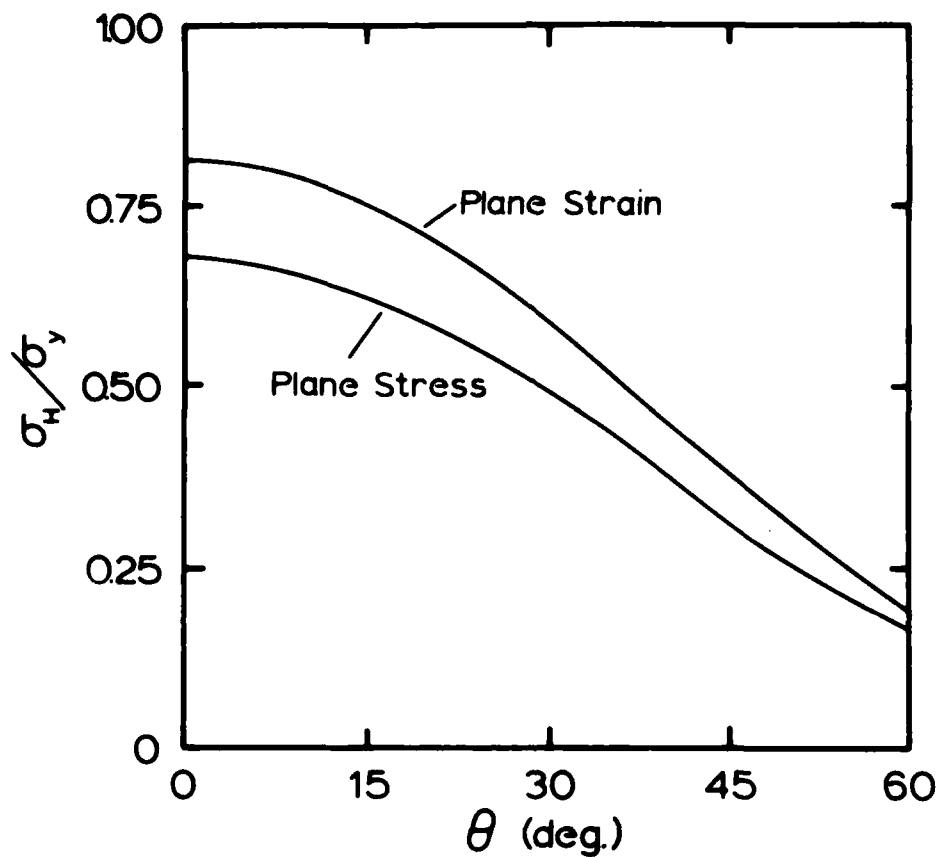


Fig. 7. The average value of σ_H/σ_y between a pair of holes as a function of hole orientation for conditions of plane strain vs. plane stress. The curves are calculated using the modified Bridgeman analysis described in the text using the lower limit value for σ_{xx} and at $\sigma_a = \sigma_y$. The plane stress values are based on $\sigma_{zz} = \sigma^* \cos^2 \theta \ln A$, using Bridgeman's relationship for σ_{zz} .¹³ Note that $(\ln A)_{Ave} = 0.493$ for $a/R = 2$.

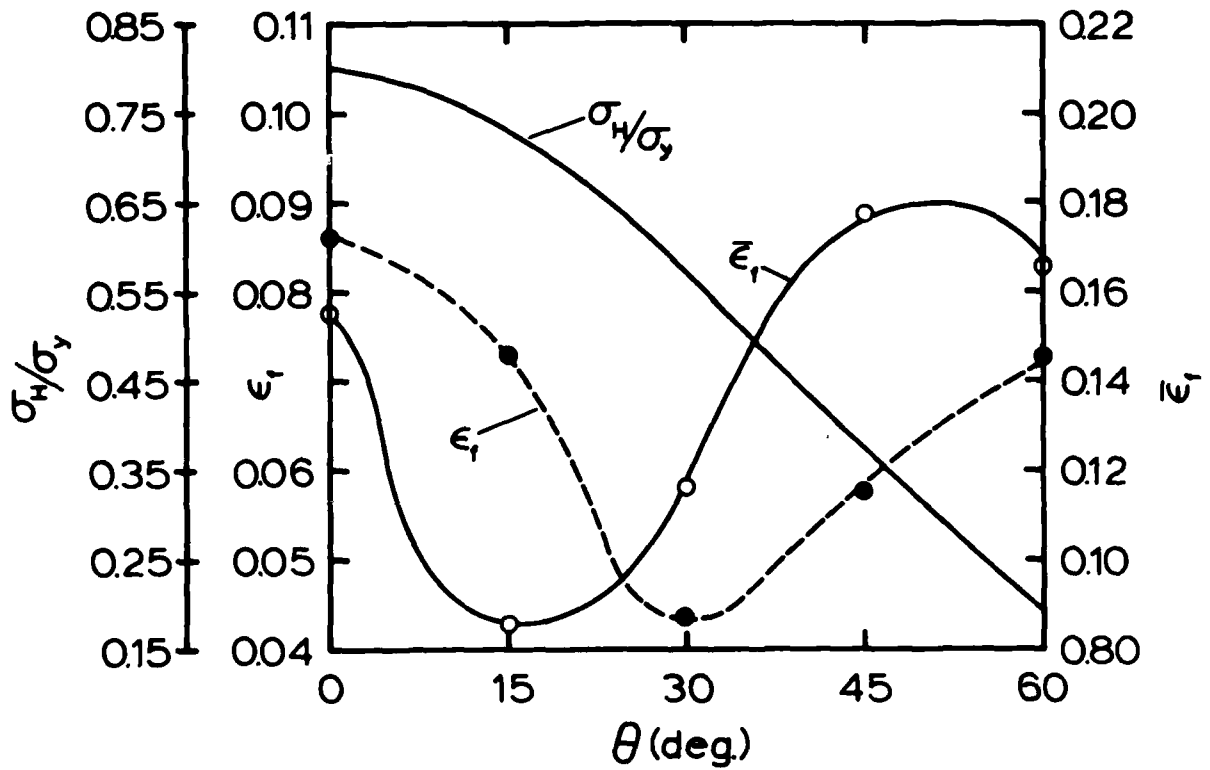


Fig. 8. The dependence of the stress ratio $\sigma_H/\bar{\sigma}$, the tensile strain to fracture ϵ_f , and the equivalent strain to fracture $\bar{\epsilon}_f$ on the hole orientation θ for a 7075 Al alloy in the T6 temper.

REPORT DOCUMENTATION PAGE		READ INSTRUCTIONS BEFORE COMPLETING FORM
1. REPORT NUMBER No. 11 ✓	2. GOVT ACCESSION NO.	3. RECIPIENT'S CATALOG NUMBER
4. TITLE (and Subtitle) 6) Ductile Fracture Under Multiaxial Stress States Between Pairs of Holes		5. TYPE OF REPORT & PERIOD COVERED
		6. PERFORMING ORG. REPORT NUMBER
7. AUTHOR(s) 10) R. J. Bourcier ● D. A. Koss		8. CONTRACT OR GRANT NUMBER(s) 15) N00014-76-C-0037
9. PERFORMING ORGANIZATION NAME AND ADDRESS Department of Metallurgical Engineering ✓ Michigan Technological University Houghton, MI 49931		10. PROGRAM ELEMENT, PROJECT, TASK AREA & WORK UNIT NUMBERS 14) TR-11
11. CONTROLLING OFFICE NAME AND ADDRESS 9) Technical Repts		12. REPORT DATE 11) Nov 79
14. MONITORING AGENCY NAME & ADDRESS (if different from Controlling Office)		13. NUMBER OF PAGES 27
		15. SECURITY CLASS. (of this report) Unclassified
		15a. DECLASSIFICATION/DOWNGRADING SCHEDULE
16. DISTRIBUTION STATEMENT (of this Report) Distribution of this document is unlimited. 12) 21		
17. DISTRIBUTION STATEMENT (of the abstract entered in Block 20, if different from Report)		
18. SUPPLEMENTARY NOTES		
19. KEY WORDS (Continue on reverse side if necessary and identify by block number) Fracture, Multiaxial Stress, Al Alloy, Void Coalescence		
20. ABSTRACT (Continue on reverse side if necessary and identify by block number) As a means of examining ductile fracture under multiaxial stress and strain states, the deformation and fracture between pairs of holes has been studied in a 7075 Al alloy. The test technique, which is unique, utilizes tensile samples each with a pair of holes through the thickness. The holes are sufficiently close (two hole diameters apart) so as to concentrate slip between them, and the local states of stress and strain can be controlled by the orientation of the holes to the stress axis. <i>over</i> (cont'd)		

20. Abstract (continued)

The influence of hole orientation on the strain at fracture has been determined in the 7075 Al alloy in the T6 as well as T0 tempers. Fracture occurs by flow localization between the holes and very little hole growth occurs, especially in the T6 condition. Fractography indicates a transition in fracture appearance with hole orientation with dimpled fracture predominating, but the degree of shear fracture increases as the pair of holes become more inclined to the stress axis. A modification of the Bridgeman analysis is used as a description of the approximate state of stress between the holes as a function of the hole orientation. The results indicated that the criterion for ductile fracture depends on both the state of stress and the strain state, but the functional dependence could not be determined. The results are also discussed as a crude model for void coalescence in ductile fracture.